

LASER APPLICATIONS AND OTHER TOPICS IN QUANTUM ELECTRONICS https://doi.org/10.1070/QEL17029

On exact determination of small radiation frequency shifts using a Fabry–Perot interferometer

A.A. Gordeev, V.F. Efimkov, I.G. Zubarev, S.I. Mikhailov

Abstract. **A method for the mathematical processing of digitised Fabry–Perot interferograms is proposed and implemented to eliminate subjective factors and increase the accuracy of measurements.**

Keywords: *Fabry–Perot etalon, frequency shift, CCD matrix, image digitisation.*

In this paper, we will focus on determining the frequency shift of spectral lines when this shift is comparable with the resolution of the measuring device. In numerous experimental studies on stimulated scattering, characterised by small frequency shifts of the scattered radiation lines relative to the lines of the exciting radiation, to record the spectra by means of the Fabry–Perot etalon, the field of view of the spectrum-recording element (film, CCD matrix) is divided into two independent areas. Each of the areas is illuminated by only one light source (usually this is pump radiation or stimulated scattering radiation; see, e.g., [1–4]). Adequate determination of the frequency shift requires accurate measurements of the diameters of the interference rings. These measurements imply that the interference pattern is divided strictly by the diameter of the rings. However, in experimental practice, such a division, of course, is carried out with some uncertainty, and this immediately introduces an error into the spectral measurements. In addition, the image of the rings has a speckled character, which makes it difficult to find the maximum of the spectral line, which will be discussed below. This paper is devoted to the development of a method for minimising these errors.

Figure 1 shows a schematic of one of the options for implementing this method. Light beams (*1*, *2*) from different sources fall on an opaque flat thin screen (*3*) and then on a lens (*4*), which forms the image of the edge of the screen at infinity. After the lens, parallel beams arrive at a Fabry–Perot etalon (*5*), and then at another lens (*6*), the focus of which is a CCD matrix (*7*). The vertical dashed line denotes the focal plane of lens *4*, in which the light-scattering element is sometimes placed to improve the uniformity of illumination of the etalon mirrors. In such scheme, a spectral picture arises at the focus of lens *6*, in one half of which is the spectrum (in the form of half-rings) of the radiation from beam *1*, and in the other from beam *2*. The CCD matrix (in our case, the WinCamD-UCM matrix of DataRay, 1020×1020 pixels) records the spectral pattern, which is usually observed on a computer monitor and processed using standard software. Note that the CCD matrix is commonly used to record the parameters of the near and far zones of laser radiation, the patterns that vary fairly smoothly along the transverse coordinate. And the standard processing methods include the determination of the intensity maxima positions, average transverse beam size, etc., using smoothing functions to construct intensity distributions in fixed sections of a 2D CCD matrix.

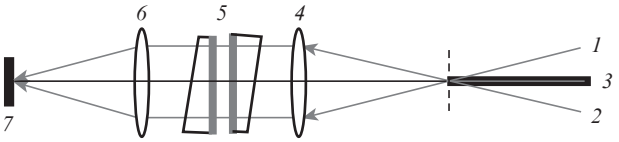

Figure 1. Optical scheme of bipolar measurement of spectra: (*1*, *2*) light beams from different sources; (*3*) screen; (*4*) lens with a focal length of 34 cm; (*5*) Fabry–Perot etalon; (*6*) lens with a focal length of 48 cm; (*7*) CCD.

On the contrary, the pattern of the intensity distribution during the registration of spectra using the Fabry–Perot etalon is, as noted above, very inhomogeneous (speckled) due to the interference of neighbouring portions of the focal image distribution at a finite aperture of the optical system, as well as by the interference of the main image with light, parasitically scattered by the elements of the optical system. This circumstance does not allow the diameters of interference rings to be correctly determined. As an example, Fig. 2 shows typical intensity distributions recorded using a CCD matrix according to the scheme shown in Fig. 1. These distributions correspond to a three-dimensional picture of the ring structure obtained using two light beams with different intensities.

To increase the accuracy of measuring the parameters of the interference pattern, it is obviously necessary to find the geometric centre of the system of interference rings and sum the radial amplitudes in a certain angle separately for the upper and lower half-planes. This procedure is equivalent to averaging over an ensemble of realisations of random phase relationships of interfering fields, i.e., the transition from coherent illumination to incoherent one.

For definiteness, we will use the programming language of the popular mathematical package Mathcad, which allows BMP and CSV files to be processed; the form of these files makes it possible to represent the results of image recording with a CCD matrix, the language itself being intuitive and concise. In the initial approximation, we introduce the centre coordinates and the radius of the circle a_0, b_0, and R_0 (the

A.A. Gordeev, V.F. Efimkov, I.G. Zubarev, S.I. Mikhailov Lebedev Physical Institute, Russian Academy of Sciences, Leninsky prosp. 53, 119991 Moscow, Russia; e-mail: mihailovsi@lebedev.ru

Received 28 March 2019
Kvantovaya Elektronika **49** (9) 878–880 (2019)
Translated by V.L. Derbov

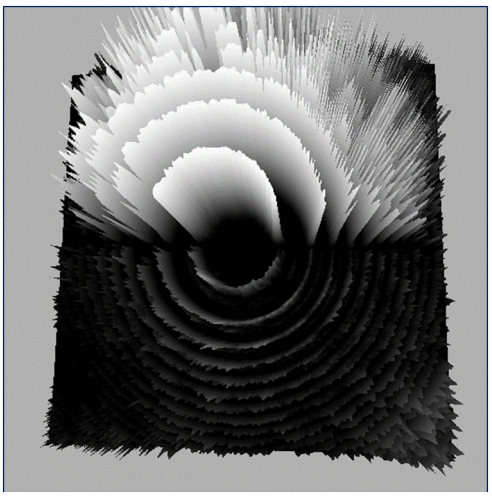

Figure 2. Illustration of the inhomogeneity (speckle) of the ring structure of the signal recorded by the CCD matrix according to the scheme shown in Fig. 1.

radius R_0 can be the approximate radius of any selected ring of the interferogram, except, obviously, the minimum one), which can be visually determined using an arbitrary graphics editor or using Mathcad. We introduce the function F(R, a, b), where a, b are the centre coordinates of the circle of radius R, of the form

$$\begin{aligned} &c := 0 \\ F(R,a,b) := &\left| \begin{array}{l} \text{for } j \in 0 .. G \\ \quad \text{for } i \in 0 .. a_0 \\ \quad\quad c \leftarrow \left| \begin{array}{l} c + A_{i,j} \ \text{ if } \left| \sqrt{(i-a)^2 + (j-b)^2} + R \right| \le h . \\ c \ \text{ otherwise} \end{array} \right. \\ \dfrac{c}{R} \end{array} \right. \end{aligned} \qquad (1)$$

Here $A_{i,j}$ is the amplitude of a signal from the pixel with coordinates i, j; 2h is the bandwidth of summation in pixels; and G is the size of the square matrix in pixels. We define the domain of variation for the discrete coordinates a, b and the radius R as $a_0 - d < a < a_0 + d$, $b_0 - d < b < b_0 + d$, $R_0 - d < R < R_0 + d$. The value of d is chosen based on simple considerations: It is necessary that the true values of the coordinates and radius surely fall into the domain of their variation. The first two lines of the program (1) define the domains of coordinate variation, the third line indicates the summation using the conditional operator: If the arguments R, a, b satisfy the condition given in (1), then the corresponding element $A_{i,j}$ is added to the sum, otherwise 0 is added. The value of the function F(R, a, b) is normalised to R, because the number of summation elements is obviously proportional to the radius R. The function F(R, a, b) is the overlap integral of a homogeneous ring having a width of $\sim 2h$ and an average radius R, with the chosen interferogram ring. Next, using the simple enumerative technique, we find the maximum of this function (this procedure is also easily implemented by means of the Mathcad software). If we choose the width 2h approximately equal to the width of the interference ring, then the corresponding values of the coordinates a and b practically coincide with the coordinates of the centre of the interference pattern (this can be understood from simple geometric considerations). Thus, using procedure (1), the coordinates a and b of the centre of the interference pattern are determined. Note that here we have chosen the upper half-plane of the matrix ($0 \leqslant i \leqslant a_0$) as the working one. The same can be done with the lower half-plane ($a_0 \leqslant i \leqslant G$), where an interferogram of another radiation is recorded.

To plot the dependence of the total signal of the pixels on the radius, we perform the summation procedure using a vector f_k of the form

$$\begin{aligned} &k := 1..3 \cdot a \qquad R_k := \frac{k}{3} \qquad c_k := 0 \\ f_k := &\left| \begin{array}{l} \text{for } j \in 0 .. G \\ \quad \text{for } i \in 0 .. a \\ \quad\quad c_k \leftarrow \left| \begin{array}{l} c_k + A_{i,j} \ \text{ if } \left| \sqrt{(i-a)^2 + (j-b)^2} + R_k \right| \le 0.5 . \\ c_k \ \text{ otherwise} \end{array} \right. \\ \dfrac{c_k}{R_k} \end{array} \right. \end{aligned} \qquad (2)$$

Here, to increase the number of calculation points by a factor of three, a discrete variable k is introduced, and the summation bandwidth is approximately one pixel. The quantities a and b correspond to the maximum of the function F(R,a,b). Similarly to Eqn (1), the magnitude of the vector f_k is normalised to R_k. As an example, Fig. 3 shows the results of processing interferograms of the second harmonic radiation of a stabilised single-mode continuous-wave Nd:YAG laser. Both recorded fields were produced by the same radiation. The dashed curve corresponds to the upper field; the solid curve corresponds to the lower one. It is clearly seen that the dependences of the intensity on the radius for both registration fields practically coincide. This is direct evidence of the correctness of the chosen method.

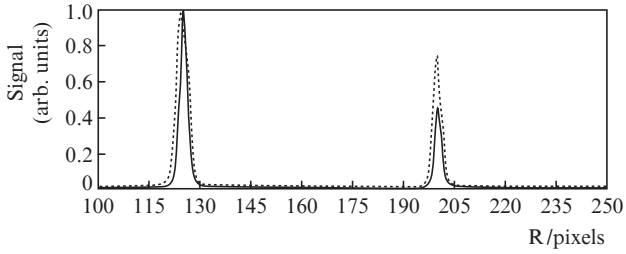

Figure 3. Results of processing interferograms of the second harmonic radiation from a stabilised single-mode continuous-wave Nd:YAG laser. The solid and dashed curves correspond to two fields of interferograms for light beams of the same frequency.

Figure 4 shows the interferogram obtained in the study of stimulated temperature scattering (STS) in the case of two-photon absorption in toluene, and the results of its processing. The second harmonic of a single-mode single-frequency Nd:glass laser, the radiation of which was focused by a lens with a focal length of 5 cm to the centre of a cell 6 cm long, served as a pump source. The pulse duration was 10 ns at its energy of 3 mJ. The gap of the modernised Fabry–Perot etalon [5] was 9 cm. The anti-Stokes shift of the scattered radiation frequency is clearly visible, which is approximately six times the theoretically obtained stationary shift $\Delta\nu = \chi q^2/2\pi \approx$ 16 MHz, where χ is the thermal diffusivity of toluene, and q is the modulus of the wave vector of the grating [6]. Thus, the method used for processing interferograms allowed us not

only to measure the spectral shifts at the limit of the resolution of the device, but also to quantitatively characterise the asymmetry of the line of stimulated temperature scattering of the pump radiation in liquid toluene.

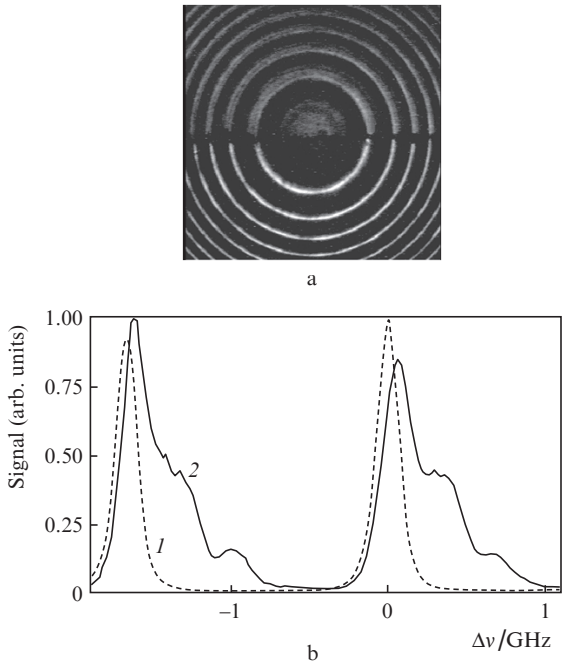

Figure 4. (a) Interferogram and (b) corresponding spectra of (*1*) pump radiation and (*2*) anti-Stokes STS component with a frequency shift of ~100 MHz, obtained as a result of mathematical processing of the first two rings.

In conclusion, we note that in order to speed up the calculations, we can introduce the corresponding restrictions on the domain of variation of the coordinates i and j, and by introducing additional conditions in Eqn (2), perform the summation in any arbitrarily given central angle containing arcs of interference rings. The coordinates of the centre of the interference pattern can be determined with greater accuracy using the half-plane where the spectrum of the pump radiation is recorded, due to its greater monochromaticity compared to scattered radiation. The considered method was used to process the results in Ref. [6].

References

1. Karpov V.B., Korobkin V.V., Dolgolenko D.A. *Sov. J. Quantum Electron.*, **21** (11), 1235 (1991) [*Kvantovaya Elektron.*, **18** (11), 1350 (1991)].
2. Averyushkin A.S., Bulychev N.A., Efimkov V.F., Erokhin A.I., Kazaryan M.A., Mikhailov S.I., Saraeva I.N., Zubarev I.G. *Laser Phys.*, **27**, 055401 (2017).
3. Erokhin A.I., Smetanin I.V., Mikhailov S.I., Bulychev N.A. *Opt. Lett.*, **43** (7), 1570 (2018).
4. Bel'dyugin I.M., Gordeev A.A., Efimkov V.F., Zubarev I.G., Mikhailov S.I., Sobolev V.B. *Quantum Electron.*, **39** (12), 1148 (2009) [*Kvantovaya Elektron.*, **39** (12), 1148 (2009)].
5. Efimkov V.F., Zubarev I.G., Mikhailov S.I. *Instrum. Exp. Tech.*, **61** (1), 114 (2018) [*Prib. Tekh. Eksp.*, (1), 100 (2018)].
6. Gordeev A.A., Efimkov V.F., Zubarev I.G., Mikhailov S.I. *Quantum Electron.*, **48** (9), 823 (2018) [*Kvantovaya Elektron.*, **48** (9), 823 (2018)].